

Celebrating
31 Years
of
Barbara Emery





1986 +

Print File
ARCHIVAL PRESERVERS

STYLE NO. 35-4 H

DATE

ASSIGNMENT

PHOTO PLASTIC PRODUCTS, INC. P.O. BOX 17638 ORLANDO, FLORIDA 32860 • (305) 896-3100

Summer · Kathryn Drake
Cedar Seminar

INSERT EMULSION SIDE DOWN

FILE NO. 7112

KODAK TX 5063

KODAK TX 5063

KODAK TX 5063

KODAK TX 5063



KODAK TX 5063

KODAK TX 5063

KODAK TX 5063

KODAK TX 5063

KODAK



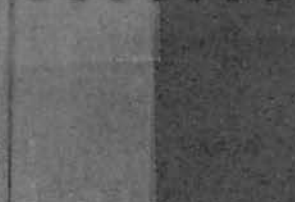
KODAK TX 5063

KODAK TX 5063

KODAK TX 5063

KODAK TX 5063

0 2 7 0 7 7 1



1987







2002



CEDAR 2002
Linda Beane
Host

CEDAR 2002
Barbara Emery
Host

SOUTH
SUMMIT

CEDAR

1998 SUMMER WORKSHOP
BOULDER, COLORADO

2002



SOUTH
SUMMIT

CEDAR

1998 SUMMIT WORKSHOP
BOULDER, COLORADO

2002



2002



2002



2003



2003

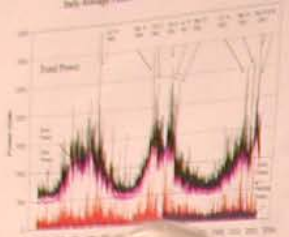


Figure 1: The winter electron energy flux as a function of IMF. Average Average flux above 60 mlat as a function of IMF and season.

$Q = \text{Pod} \times \text{IMF}$

We compare the cross-correlation coefficient (CC) to estimate whether or not the two series are statistically independent. We also compare the cross-correlation coefficient to the Pearson correlation coefficient.

Dynamic Explorer-2 Data:

Data from 172 days (from day 261 1991 to day 41 1994), during winter maximum when the IMF was from 200 to 110. Periods through 17 to 1 June 2001 usually represent polar storms combined with highly IMF.

LAPs electron precipitation gives electron flux (EF) and mean electron energy (EE) Data by Solar wind and Magnetospheric parameters:

total $\text{Pod} = \text{speed}(v) \times 20 \times \text{Dx} / (4\pi r^2)$
 winter $\text{Pod} = 11 \times 0.14 \times \text{polar width angle}$
 $\text{Pod} = \text{speed} \times \text{Pod}^2 \times \text{cos}(\text{Pod}^2)$
 IMF (magnetospheric) and RPA give us IMF (IMF)

IMF gives 8 mlat for Poynting vector (CVS of IMF)

CM and 2.5 mlat above 41 mlat for 1 and 2.5 mlat resolution with variable MLT resolution to obtain from about 300 and 240 km square. Averages were calculated above 60 mlat in 12 or 200 km. Pod are for 2.5 mlat unless otherwise stated.

Imaged in IMF (By, Bz, By) and dipole (W winter), (summer and summer) Combined northern (N) and southern (S) hemispheres

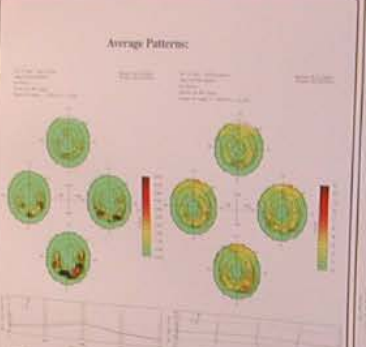


Figure 2: The winter total electron energy flux as a function of IMF. Average Average flux above 60 mlat as a function of IMF and season.

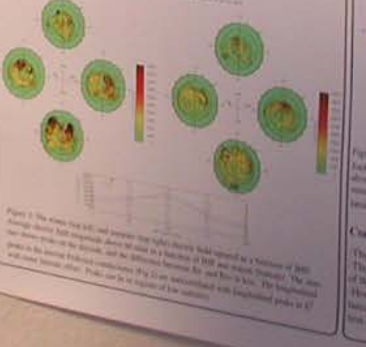


Figure 3: The winter total electron energy flux as a function of IMF. Average Average flux above 60 mlat as a function of IMF and season.

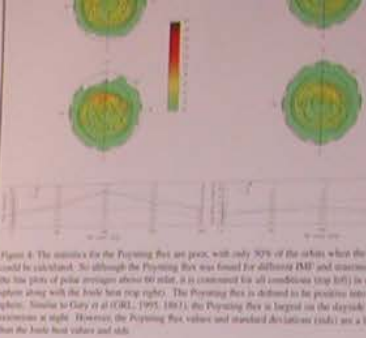


Figure 4: The statistics for the Poynting flux are poor, with only 30% of the values when the total heat could be calculated. So although the Poynting flux was found for different IMF and seasons, as shown in the line plots of polar averages above 60 mlat, it is contained for all conditions (top left) in each hemisphere along with the total heat (top right). The Poynting flux is defined to be positive into the hemisphere. Similar to Gary et al (GRL, 1995, 1991) the Poynting flux is largest in the dayside with several exceptions at night. However the Poynting flux values and standard deviation (std) are a little larger than the total heat values and std.

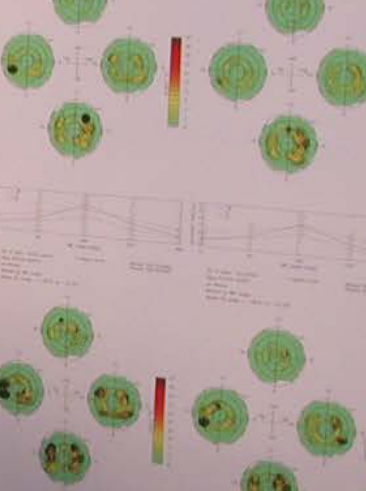


Figure 5: The winter total heat for all series (top left) and standard deviation (bottom left), and the winter total heat as a function of IMF angle and season (top right) as a function of IMF, with polar averages (bottom right), with the largest average in summer (S). It is on the left. The winter is larger and the heat from the side of E^7 and PIA, with or without the cross-correlation coefficient, Q^2 similar to E^7 .

Conclusions:

The Poynting vector is larger than the total heat in both winter and standard deviation. The standard deviation of total heat is much larger than winter and standard deviation. However, this means it is not due to the cross-correlation between the Poynting vector and the electron field against these two series because it does not decrease the standard deviation, but only slightly on the standard deviation.

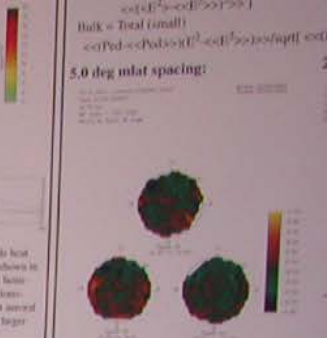


Figure 6: Cross-correlation between E^7 and Pod for By. For small cross-correlation, summer is left polar plot, winter is right in total. Line plots are for winter (W), summer (S) and summer (S) as a function of IMF angle.

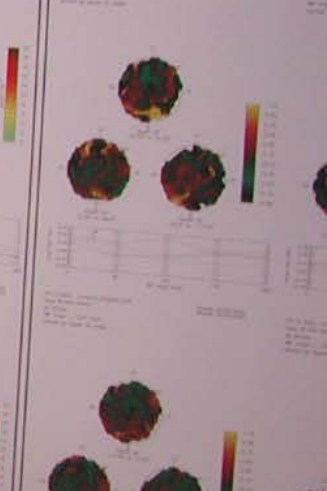


Figure 7: Small scale cross-correlation (+) equatorward of several polar cap, with size above 60 mlat of about 0.00 in summer, 0.00, smaller than 2.5 mlat shows more negative correlation. Winter polar areas are about 0.01 lower with 2.5 mlat for both (total) cross-correlation smaller. Effect on total heat to equally reduce the std on the down side (-cor), and increase

2003

Joule Heat Calculations, Standard Deviations and Cross-Correlations Derived from the Dynamics Explorer-1 Satellite

Barbara Emery and Arthur Richmond, HSONCAR

Objectives:
 Spacing the ground-based, double-beam (DB) measurements to the orbit footprint and measuring (DB) and the spacing of the double-beam (DB) measurements.

$QJ = P_{db} \times (DB)^2$

We examine the cross-correlation of Joule Heat and (DB) to estimate whether or not the cross-correlation is significant. We also compare the double-beam calculations to the Precipitating Ionospheric (PI) calculations.

Dynamics Explorer-1 Data:
 Data from 1981-1982, from July 1981 to May 1982, during solar maximum when the satellite was in orbit from 200 to 1200 km altitude through 1.1 to 7.0 AU. The satellite was in orbit with nearly 5000 orbits.

Joule Heat, Precipitating Flux and Standard Deviations

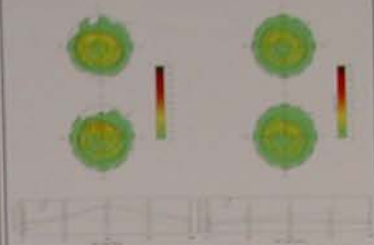


Figure 1: The results for the Precipitating Ionospheric (PI) and the double-beam (DB) calculations. The double-beam (DB) calculations are based on the double-beam (DB) and the double-beam (DB) calculations. The double-beam (DB) calculations are based on the double-beam (DB) and the double-beam (DB) calculations. The double-beam (DB) calculations are based on the double-beam (DB) and the double-beam (DB) calculations.

Cross-Correlations

Correlation in time of 1 orbit. The correlation in time of 1 orbit is calculated as follows:
 $Correlation = \frac{\sum (DB_i - \bar{DB})(PI_i - \bar{PI})}{\sqrt{\sum (DB_i - \bar{DB})^2 \sum (PI_i - \bar{PI})^2}}$

Large values indicate high correlation. Positive values indicate that the double-beam (DB) and the double-beam (DB) calculations are in phase. Negative values indicate that the double-beam (DB) and the double-beam (DB) calculations are out of phase.

1.8 deg orbit spacing 2.2 deg orbit spacing



Figure 2: The results for the cross-correlation of the double-beam (DB) and the double-beam (DB) calculations. The double-beam (DB) calculations are based on the double-beam (DB) and the double-beam (DB) calculations. The double-beam (DB) calculations are based on the double-beam (DB) and the double-beam (DB) calculations.

The double-beam (DB) calculations are based on the double-beam (DB) and the double-beam (DB) calculations. The double-beam (DB) calculations are based on the double-beam (DB) and the double-beam (DB) calculations. The double-beam (DB) calculations are based on the double-beam (DB) and the double-beam (DB) calculations.



Figure 3: The results for the double-beam (DB) and the double-beam (DB) calculations. The double-beam (DB) calculations are based on the double-beam (DB) and the double-beam (DB) calculations. The double-beam (DB) calculations are based on the double-beam (DB) and the double-beam (DB) calculations.

Conclusions:
 The double-beam (DB) calculations are based on the double-beam (DB) and the double-beam (DB) calculations. The double-beam (DB) calculations are based on the double-beam (DB) and the double-beam (DB) calculations. The double-beam (DB) calculations are based on the double-beam (DB) and the double-beam (DB) calculations.



1995 SUMMER WORKSHOP
 BOULDER, COLORADO



Flood in Snowmass 2003



2003



2003



2004



2004



2004

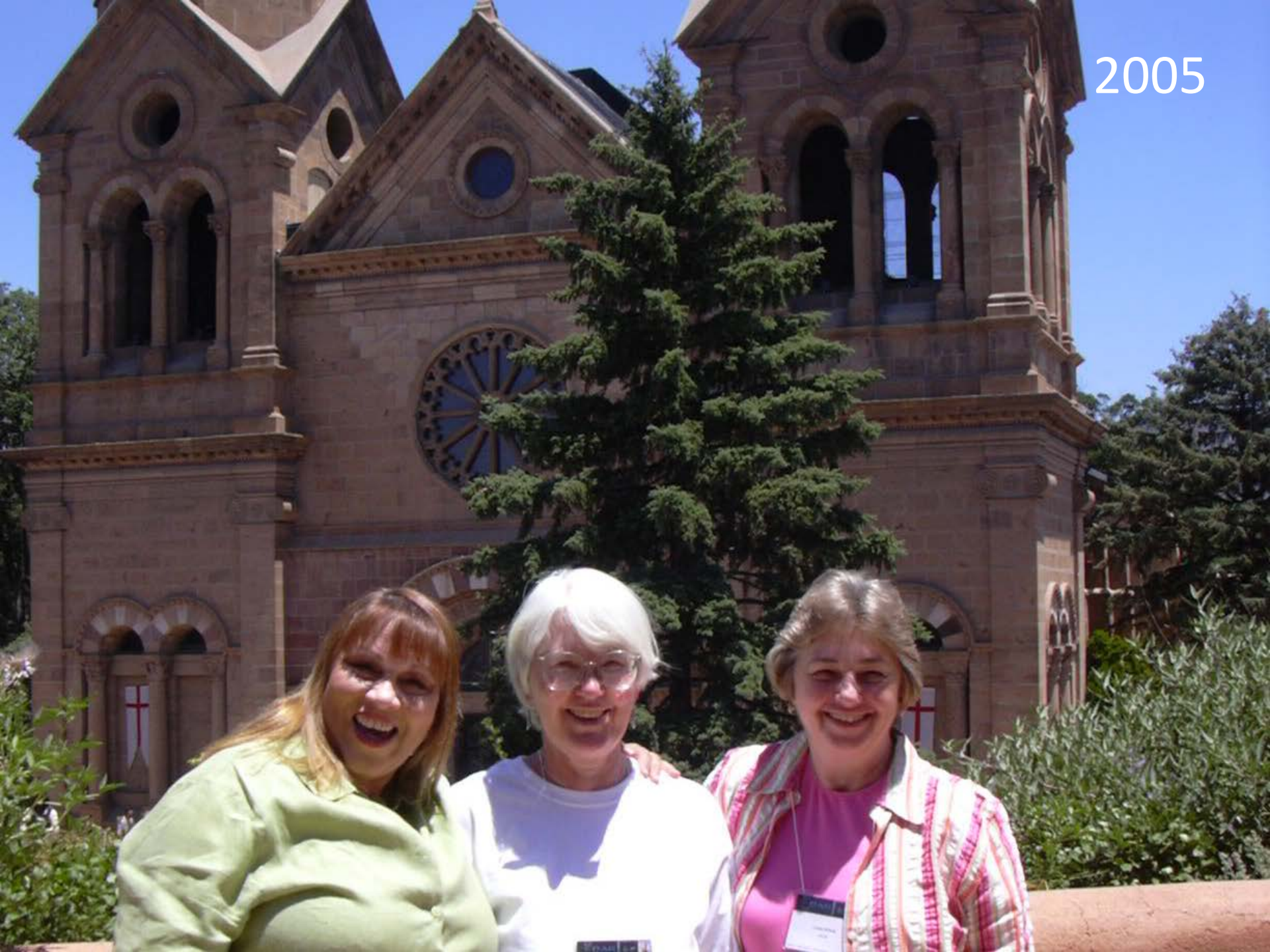


2005



2005

2005





2005



Leadville, Colorado & Southern
Railroad Company

Garrison

Michael Colwell
Leadville, Colorado & Southern Railroad Company

2005



2006



2006

EXIT



2006



2006



2006



2006



2006



2007
SANTA FE, NM

CEDAR-DASI



High altitude Interferometer WIND observations

Qian Wu

High Altitude Observatory, National Center for Atmospheric Research
Boulder, CO 80507-2009

WIND System Schematic



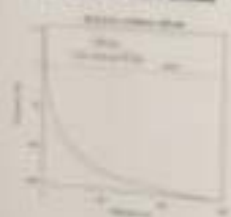
FPI Component Diagram



WIND Images at 500 level and 8000



Wind Error vs. Balloon Altitude



IGOs and SuperDARN Coverage

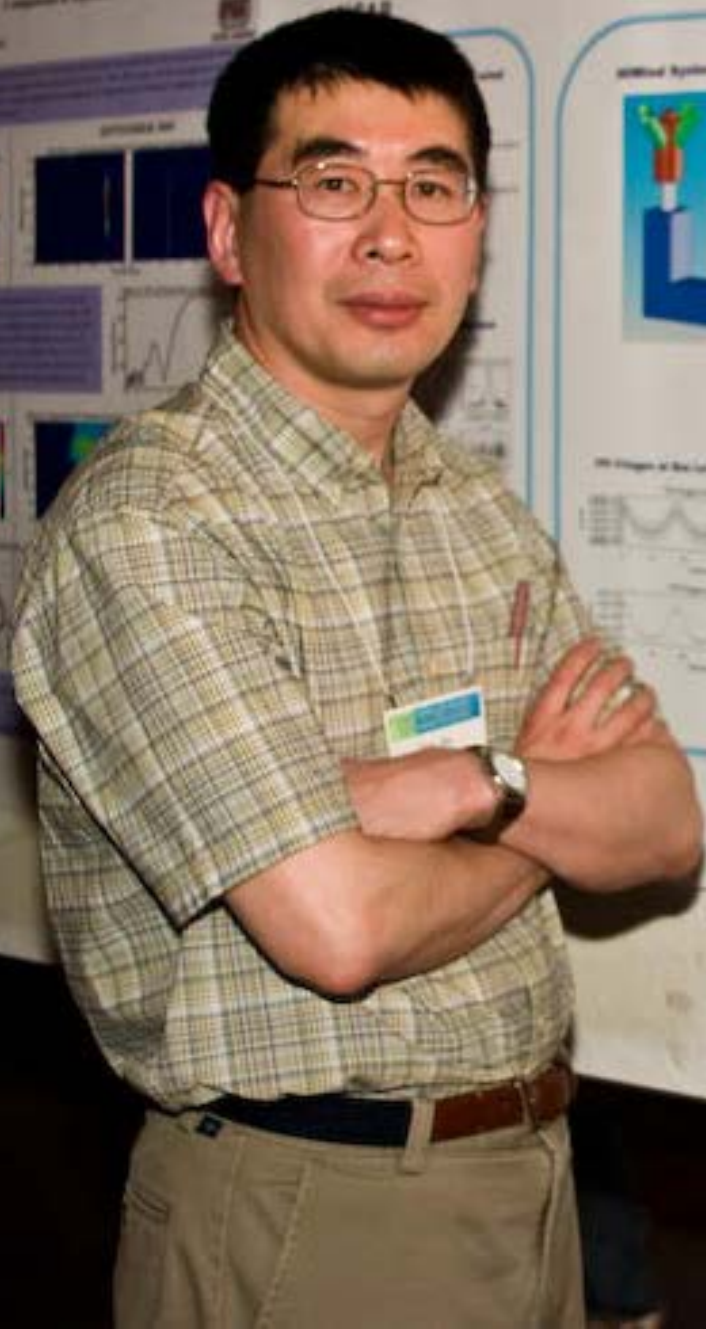


IGOs



Summary

Summary text describing the project and observations.

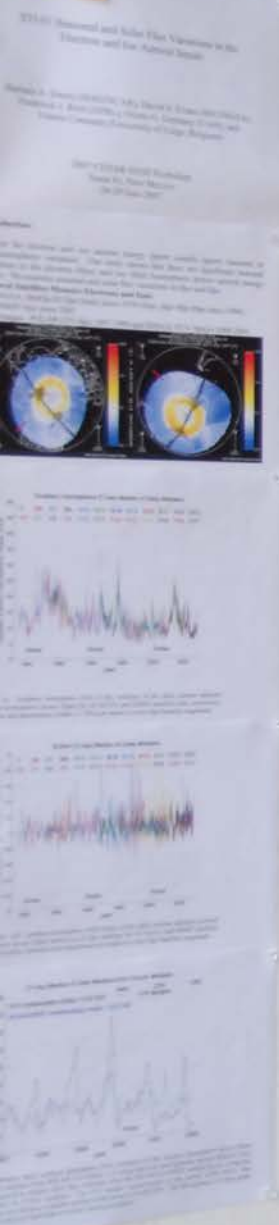



2007

2007



II-01






Effects of Auroral Precipitation on High-Latitude Ion Upwelling

M.A. Danielides, D. Lummerzheim, and A. Otto

Geophysical Institute / University of Alaska Fairbanks, 903 Koyukuk Dr., P.O. Box 757120, Fairbanks, AK 99775-7120




ABSTRACT

The ionosphere is the primary detector and detector of solar and cosmic ray activity in the upper atmosphere. As a result of its high conductivity, it is a natural barrier to the flow of ionospheric energy, and it is also a natural barrier to the flow of ionospheric energy. The ionosphere is a natural barrier to the flow of ionospheric energy, and it is also a natural barrier to the flow of ionospheric energy. The ionosphere is a natural barrier to the flow of ionospheric energy, and it is also a natural barrier to the flow of ionospheric energy.

Statistical Examination and Results

The data were analyzed for the years 1997-2000. The results show that the ionosphere is a natural barrier to the flow of ionospheric energy, and it is also a natural barrier to the flow of ionospheric energy. The ionosphere is a natural barrier to the flow of ionospheric energy, and it is also a natural barrier to the flow of ionospheric energy.



Conclusions and Results

The results show that the ionosphere is a natural barrier to the flow of ionospheric energy, and it is also a natural barrier to the flow of ionospheric energy. The ionosphere is a natural barrier to the flow of ionospheric energy, and it is also a natural barrier to the flow of ionospheric energy.



2007

2007





2007



RES & TO EC SCENI
403 1993

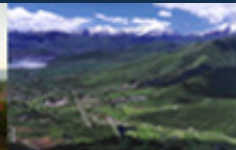
CEDAR SCGSTEP
2001
A SPACE SCIENCE ODYSSEY

2007

CEDAR
2008



June 16 - 21



Zermatt Resort



Midway, Utah





2008



2008

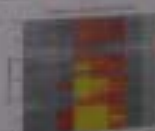


LTRV-06

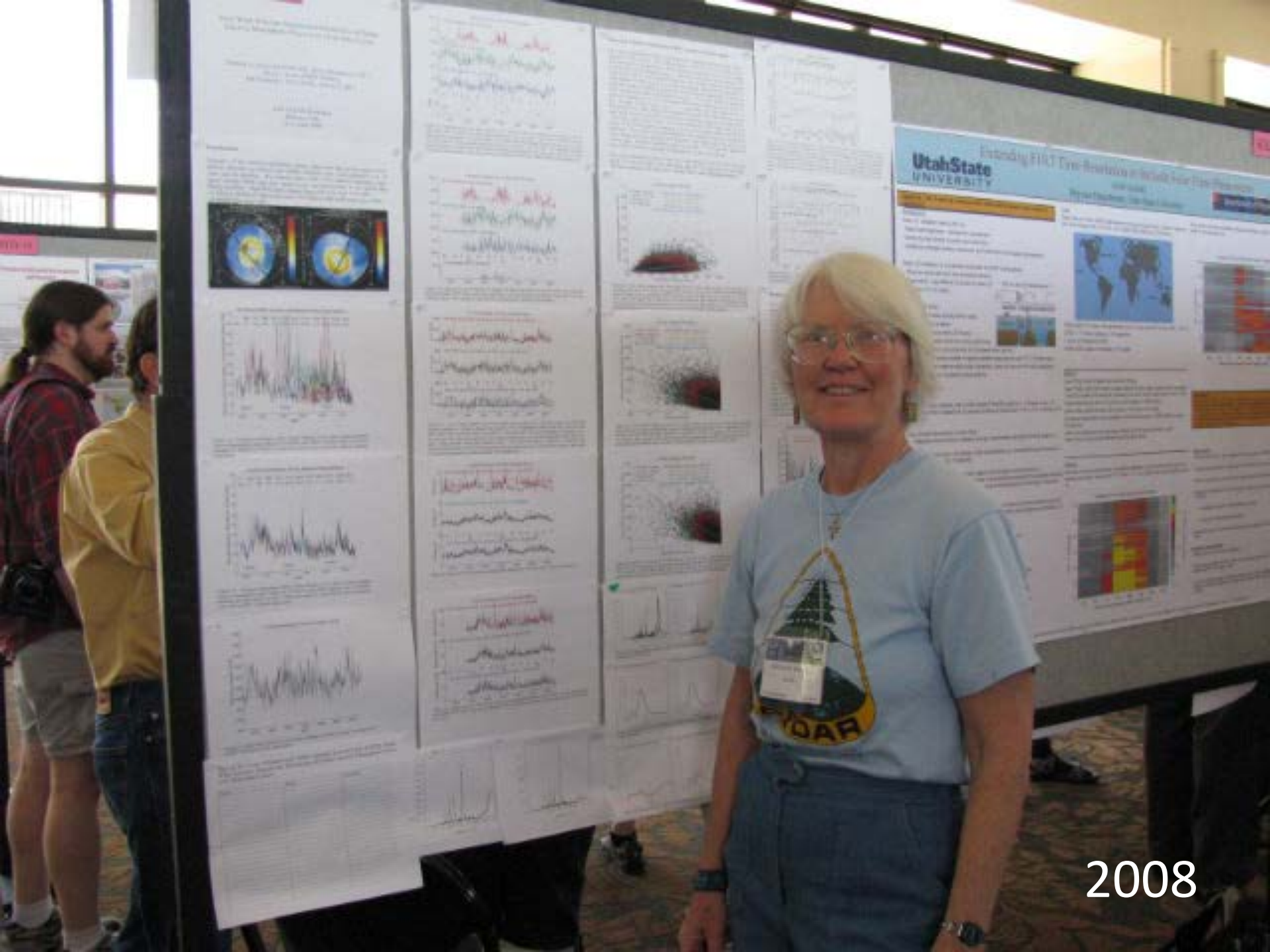


Utah State
UNIVERSITY

Estimating ERT from Reservoir Artifacts from Time



2008



2008



2008



2008



Leedville (Alabama) ...
ahead, Carolina

2008

2008



START



SALT LAKE 2002
OLYMPIC GAMES

©1994 SLOC 28 USC 505

1-1 AIRLINE SHOP

12-01 NPL WINTER

Delta



2008



2008

2008





June 28 - July 2
Eldorado Hotel Santa Fe, New Mexico



EXIT



2009



2010
CEDAR
25th ANNIVERSARY

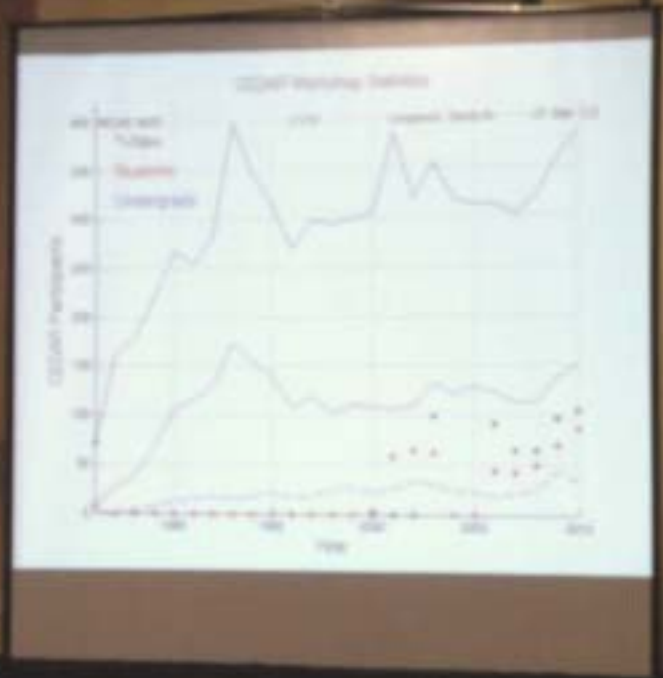
20-25 June, 2010- Boulder, Colorado



2010



2010



2010



2010





2010



2010



2010



2010
CEDAR
25th ANNIVERSARY

Barbara A. Emery
NCAR HQ
© 2010 Cedar, 2010 Boulder, Colorado





2010



2010



2010



UTKV-01

11 For Evidence and
12 Peaks During the Last
13 Solar Minimum and
14 Revised Model

Ennis WCMU, James D. ...
15 16 17 18 19 20 21 22 23 24 25 26 27 28 29 30 31 32 33 34 35 36 37 38 39 40 41 42 43 44 45 46 47 48 49 50 51 52 53 54 55 56 57 58 59 60 61 62 63 64 65 66 67 68 69 70 71 72 73 74 75 76 77 78 79 80 81 82 83 84 85 86 87 88 89 90 91 92 93 94 95 96 97 98 99 100

ABSTRACT

The solar cycle is a ...
11 12 13 14 15 16 17 18 19 20 21 22 23 24 25 26 27 28 29 30 31 32 33 34 35 36 37 38 39 40 41 42 43 44 45 46 47 48 49 50 51 52 53 54 55 56 57 58 59 60 61 62 63 64 65 66 67 68 69 70 71 72 73 74 75 76 77 78 79 80 81 82 83 84 85 86 87 88 89 90 91 92 93 94 95 96 97 98 99 100

The solar cycle is a ...
11 12 13 14 15 16 17 18 19 20 21 22 23 24 25 26 27 28 29 30 31 32 33 34 35 36 37 38 39 40 41 42 43 44 45 46 47 48 49 50 51 52 53 54 55 56 57 58 59 60 61 62 63 64 65 66 67 68 69 70 71 72 73 74 75 76 77 78 79 80 81 82 83 84 85 86 87 88 89 90 91 92 93 94 95 96 97 98 99 100



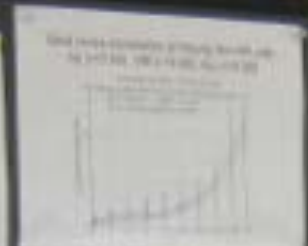
The solar cycle is a ...
11 12 13 14 15 16 17 18 19 20 21 22 23 24 25 26 27 28 29 30 31 32 33 34 35 36 37 38 39 40 41 42 43 44 45 46 47 48 49 50 51 52 53 54 55 56 57 58 59 60 61 62 63 64 65 66 67 68 69 70 71 72 73 74 75 76 77 78 79 80 81 82 83 84 85 86 87 88 89 90 91 92 93 94 95 96 97 98 99 100



The solar cycle is a ...
11 12 13 14 15 16 17 18 19 20 21 22 23 24 25 26 27 28 29 30 31 32 33 34 35 36 37 38 39 40 41 42 43 44 45 46 47 48 49 50 51 52 53 54 55 56 57 58 59 60 61 62 63 64 65 66 67 68 69 70 71 72 73 74 75 76 77 78 79 80 81 82 83 84 85 86 87 88 89 90 91 92 93 94 95 96 97 98 99 100

The solar cycle is a ...
11 12 13 14 15 16 17 18 19 20 21 22 23 24 25 26 27 28 29 30 31 32 33 34 35 36 37 38 39 40 41 42 43 44 45 46 47 48 49 50 51 52 53 54 55 56 57 58 59 60 61 62 63 64 65 66 67 68 69 70 71 72 73 74 75 76 77 78 79 80 81 82 83 84 85 86 87 88 89 90 91 92 93 94 95 96 97 98 99 100

The solar cycle is a ...
11 12 13 14 15 16 17 18 19 20 21 22 23 24 25 26 27 28 29 30 31 32 33 34 35 36 37 38 39 40 41 42 43 44 45 46 47 48 49 50 51 52 53 54 55 56 57 58 59 60 61 62 63 64 65 66 67 68 69 70 71 72 73 74 75 76 77 78 79 80 81 82 83 84 85 86 87 88 89 90 91 92 93 94 95 96 97 98 99 100



27-Day Average, 1972-2010
11 12 13 14 15 16 17 18 19 20 21 22 23 24 25 26 27 28 29 30 31 32 33 34 35 36 37 38 39 40 41 42 43 44 45 46 47 48 49 50 51 52 53 54 55 56 57 58 59 60 61 62 63 64 65 66 67 68 69 70 71 72 73 74 75 76 77 78 79 80 81 82 83 84 85 86 87 88 89 90 91 92 93 94 95 96 97 98 99 100

Local-Time, 27-Day Average
11 12 13 14 15 16 17 18 19 20 21 22 23 24 25 26 27 28 29 30 31 32 33 34 35 36 37 38 39 40 41 42 43 44 45 46 47 48 49 50 51 52 53 54 55 56 57 58 59 60 61 62 63 64 65 66 67 68 69 70 71 72 73 74 75 76 77 78 79 80 81 82 83 84 85 86 87 88 89 90 91 92 93 94 95 96 97 98 99 100



27-Day Average, 1972-2010
11 12 13 14 15 16 17 18 19 20 21 22 23 24 25 26 27 28 29 30 31 32 33 34 35 36 37 38 39 40 41 42 43 44 45 46 47 48 49 50 51 52 53 54 55 56 57 58 59 60 61 62 63 64 65 66 67 68 69 70 71 72 73 74 75 76 77 78 79 80 81 82 83 84 85 86 87 88 89 90 91 92 93 94 95 96 97 98 99 100

Local-Time, 27-Day Average
11 12 13 14 15 16 17 18 19 20 21 22 23 24 25 26 27 28 29 30 31 32 33 34 35 36 37 38 39 40 41 42 43 44 45 46 47 48 49 50 51 52 53 54 55 56 57 58 59 60 61 62 63 64 65 66 67 68 69 70 71 72 73 74 75 76 77 78 79 80 81 82 83 84 85 86 87 88 89 90 91 92 93 94 95 96 97 98 99 100

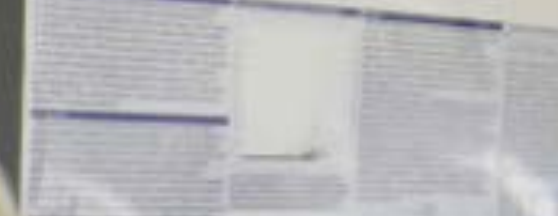
11 12 13 14 15 16 17 18 19 20 21 22 23 24 25 26 27 28 29 30 31 32 33 34 35 36 37 38 39 40 41 42 43 44 45 46 47 48 49 50 51 52 53 54 55 56 57 58 59 60 61 62 63 64 65 66 67 68 69 70 71 72 73 74 75 76 77 78 79 80 81 82 83 84 85 86 87 88 89 90 91 92 93 94 95 96 97 98 99 100

11 12 13 14 15 16 17 18 19 20 21 22 23 24 25 26 27 28 29 30 31 32 33 34 35 36 37 38 39 40 41 42 43 44 45 46 47 48 49 50 51 52 53 54 55 56 57 58 59 60 61 62 63 64 65 66 67 68 69 70 71 72 73 74 75 76 77 78 79 80 81 82 83 84 85 86 87 88 89 90 91 92 93 94 95 96 97 98 99 100

11 12 13 14 15 16 17 18 19 20 21 22 23 24 25 26 27 28 29 30 31 32 33 34 35 36 37 38 39 40 41 42 43 44 45 46 47 48 49 50 51 52 53 54 55 56 57 58 59 60 61 62 63 64 65 66 67 68 69 70 71 72 73 74 75 76 77 78 79 80 81 82 83 84 85 86 87 88 89 90 91 92 93 94 95 96 97 98 99 100

11 12 13 14 15 16 17 18 19 20 21 22 23 24 25 26 27 28 29 30 31 32 33 34 35 36 37 38 39 40 41 42 43 44 45 46 47 48 49 50 51 52 53 54 55 56 57 58 59 60 61 62 63 64 65 66 67 68 69 70 71 72 73 74 75 76 77 78 79 80 81 82 83 84 85 86 87 88 89 90 91 92 93 94 95 96 97 98 99 100

11 12 13 14 15 16 17 18 19 20 21 22 23 24 25 26 27 28 29 30 31 32 33 34 35 36 37 38 39 40 41 42 43 44 45 46 47 48 49 50 51 52 53 54 55 56 57 58 59 60 61 62 63 64 65 66 67 68 69 70 71 72 73 74 75 76 77 78 79 80 81 82 83 84 85 86 87 88 89 90 91 92 93 94 95 96 97 98 99 100



11 12 13 14 15 16 17 18 19 20 21 22 23 24 25 26 27 28 29 30 31 32 33 34 35 36 37 38 39 40 41 42 43 44 45 46 47 48 49 50 51 52 53 54 55 56 57 58 59 60 61 62 63 64 65 66 67 68 69 70 71 72 73 74 75 76 77 78 79 80 81 82 83 84 85 86 87 88 89 90 91 92 93 94 95 96 97 98 99 100

11 12 13 14 15 16 17 18 19 20 21 22 23 24 25 26 27 28 29 30 31 32 33 34 35 36 37 38 39 40 41 42 43 44 45 46 47 48 49 50 51 52 53 54 55 56 57 58 59 60 61 62 63 64 65 66 67 68 69 70 71 72 73 74 75 76 77 78 79 80 81 82 83 84 85 86 87 88 89 90 91 92 93 94 95 96 97 98 99 100



11 12 13 14 15 16 17 18 19 20 21 22 23 24 25 26 27 28 29 30 31 32 33 34 35 36 37 38 39 40 41 42 43 44 45 46 47 48 49 50 51 52 53 54 55 56 57 58 59 60 61 62 63 64 65 66 67 68 69 70 71 72 73 74 75 76 77 78 79 80 81 82 83 84 85 86 87 88 89 90 91 92 93 94 95 96 97 98 99 100

2010



2010

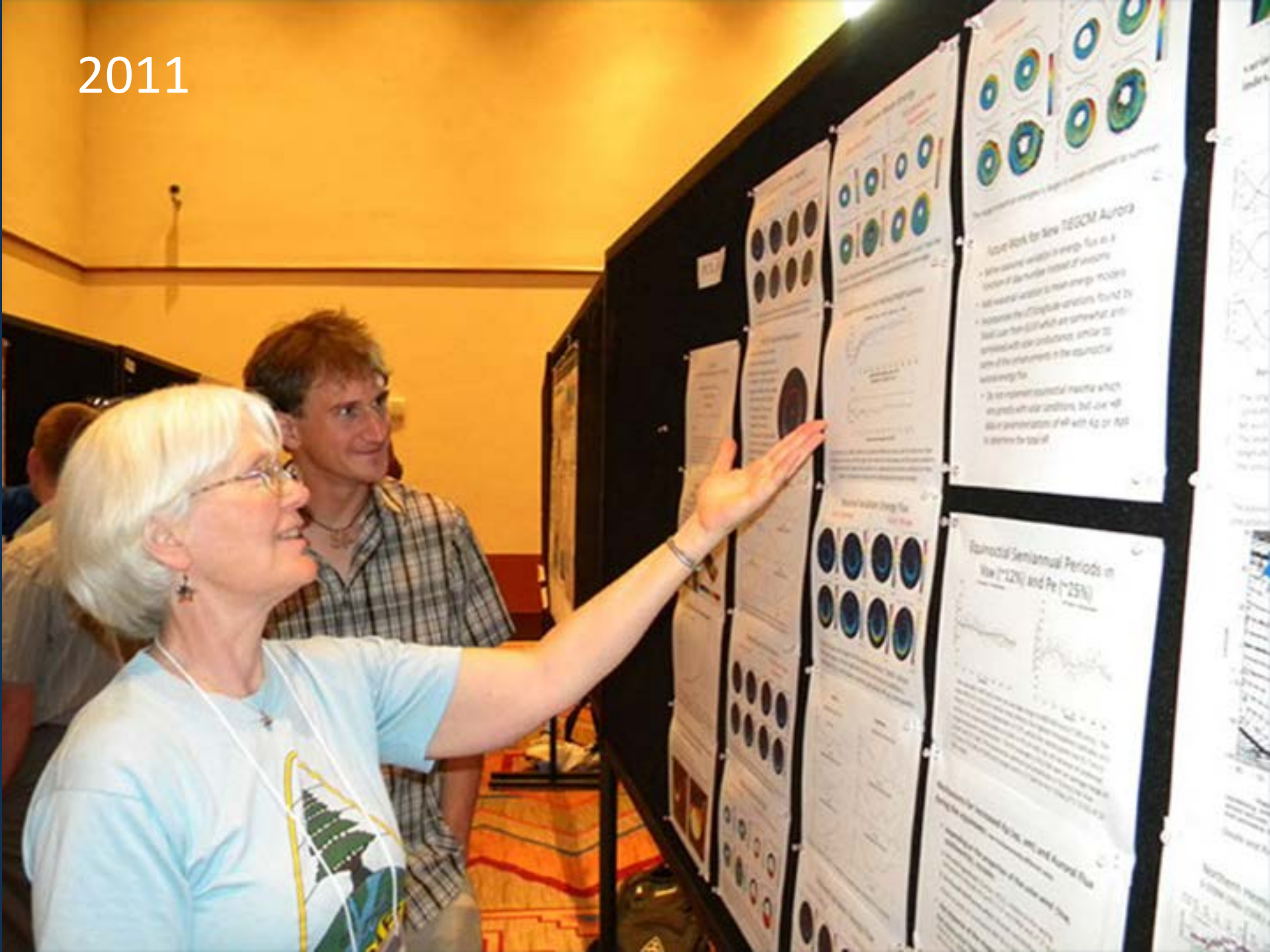


CEDAR-GEM JOINT WORKSHOP



26 JUNE - 1 JULY 2011 ~ SANTA FE, NEW MEXICO

2011



Low Work for Slow TECM Aurora

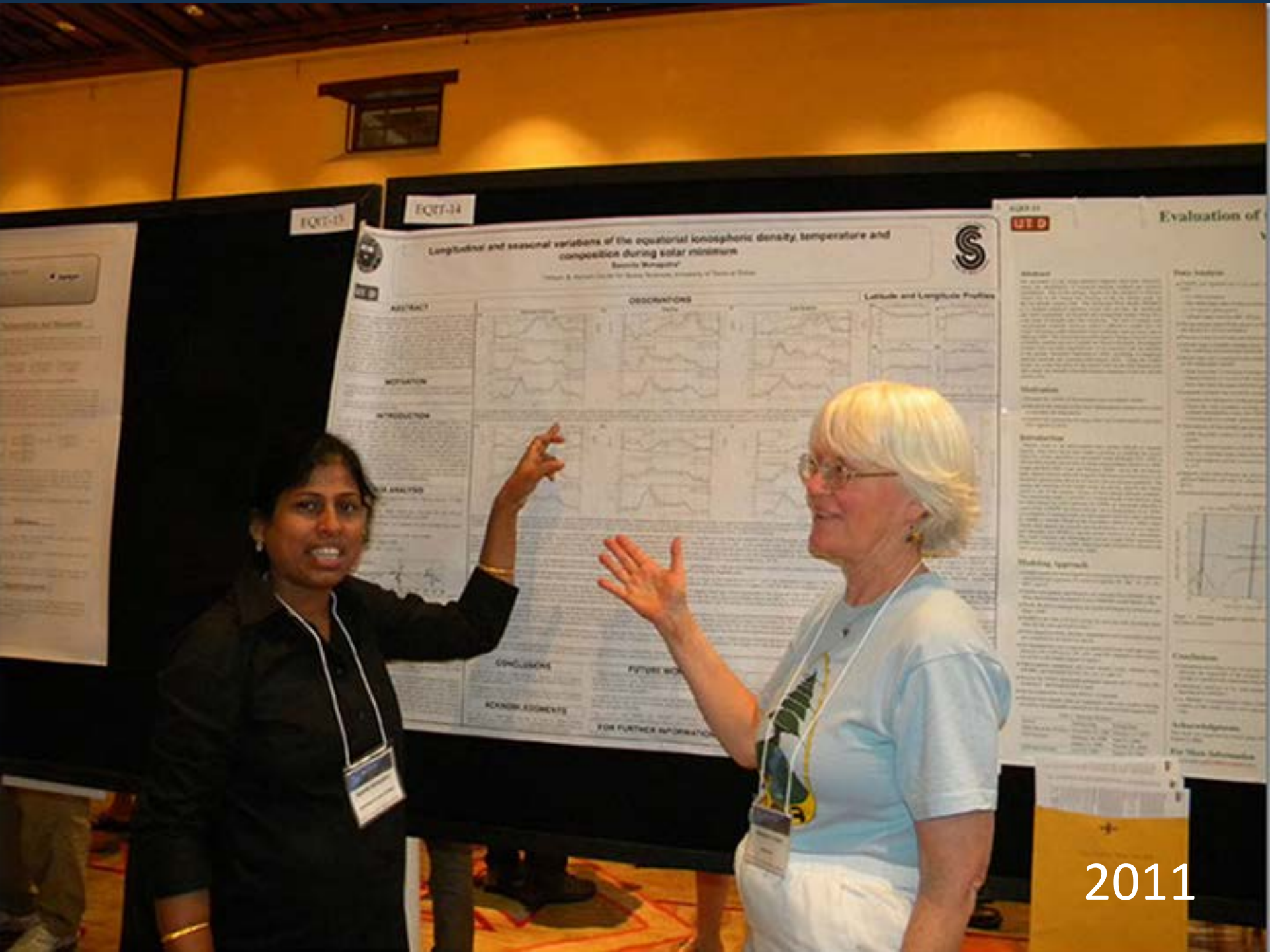
- A low amount of energy flux as a fraction of the total energy flux
- A low amount of energy flux as a fraction of the total energy flux
- A low amount of energy flux as a fraction of the total energy flux
- A low amount of energy flux as a fraction of the total energy flux

Equinoctial Semiannual Periods in Wk (~12%) and Fe (~25%)





2011



Longitudinal and seasonal variations of the equatorial ionospheric density, temperature and composition during solar minimum
Savitri Wangathir



ABSTRACT

MOTIVATION

INTRODUCTION

DATA ANALYSIS

OBSERVATIONS

Latitude and Longitude Profiles

CONCLUSIONS

FUTURE WORK

ACKNOWLEDGMENTS

FOR FURTHER INFORMATION

UTD

Evaluation of

2011



2011

CEDAR

2012



June 24 - June 29

Eldorado Hotel Santa Fe, New Mexico





2012

Climatology Assessment of Ionosphere/Thermosphere Models in Low Solar Flux Conditions for the CCMC CEDAR Challenge

84 Emery, J. D. (1), G. Keckman, C. Willes, J. Chau, G. Crowley, M. Castellano, A. Coiro, J. F. Emmert, M. Healy, R. F. Healy, T. A. Kuster, M. L. M. de Almeida, S. Bracher, J. H. Chou, J. L. Chau, A. M. MacLeod, S. McPherson, J. P. R. de Almeida, C. Scherer, A. Schuck, J. Sola, D. Thompson, J. Sutton, G. Weimer, G. Wu
 CCMC, SOLA-06, 26 June 2012, Santa Fe, NM

Global or 2-D or 3-D or CCMF Neutral Density at 400 km

There are professional grade 3-D data sets of the high-latitude solar wind velocity (SWV) and the CCMF neutral density at 400 km. These data sets are used to compare the CCMF neutral density at 400 km to the SWV data. The CCMF neutral density at 400 km is compared to the SWV data at 400 km. The CCMF neutral density at 400 km is compared to the SWV data at 400 km. The CCMF neutral density at 400 km is compared to the SWV data at 400 km.

Daily TEC (global and lon-24h)

Two panels show the weighted global and local TEC for the 24h period. The global TEC is shown in the top panel and the local TEC is shown in the bottom panel. The global TEC is shown in the top panel and the local TEC is shown in the bottom panel. The global TEC is shown in the top panel and the local TEC is shown in the bottom panel.

Comparison of MIT and IGS TEC

IGS TEC data are compared to MIT TEC data. The IGS TEC data are shown in the top panel and the MIT TEC data are shown in the bottom panel. The IGS TEC data are shown in the top panel and the MIT TEC data are shown in the bottom panel.

CCMC Electrodynamics-Ionosphere-Thermosphere Challenge

The CCMC Electrodynamics-Ionosphere-Thermosphere Challenge (EIT) Challenge selected several (10) teams and the year of the challenge (March 2012 - March 2013) for the challenge of the first CEDAR EIT Challenge Workshop in the summer of 2012. We selected solar minimum conditions (2009-2010) for the challenge. The challenge was held in Santa Fe, NM, and the challenge was held in Santa Fe, NM. The challenge was held in Santa Fe, NM, and the challenge was held in Santa Fe, NM.

Solar Wind TEC and Density

The challenge was held in Santa Fe, NM, and the challenge was held in Santa Fe, NM. The challenge was held in Santa Fe, NM, and the challenge was held in Santa Fe, NM. The challenge was held in Santa Fe, NM, and the challenge was held in Santa Fe, NM.

Summary of MIT TEC Climatology

The MIT TEC climatology is shown in the top panel. The MIT TEC climatology is shown in the top panel. The MIT TEC climatology is shown in the top panel. The MIT TEC climatology is shown in the top panel.

Summary of COSMIC NmF2 Climatology

The COSMIC NmF2 climatology is shown in the top panel. The COSMIC NmF2 climatology is shown in the top panel. The COSMIC NmF2 climatology is shown in the top panel. The COSMIC NmF2 climatology is shown in the top panel.

Summary of COSMIC HmF2 Climatology

The COSMIC HmF2 climatology is shown in the top panel. The COSMIC HmF2 climatology is shown in the top panel. The COSMIC HmF2 climatology is shown in the top panel. The COSMIC HmF2 climatology is shown in the top panel.

Summary of the First CCMC Climatology Study

The first CCMC climatology study is shown in the top panel. The first CCMC climatology study is shown in the top panel. The first CCMC climatology study is shown in the top panel. The first CCMC climatology study is shown in the top panel.

Future Participants

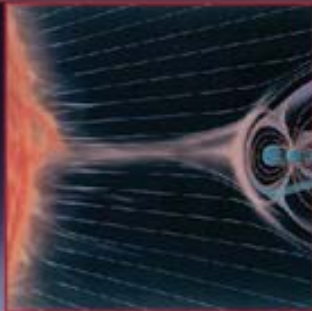
The future participants are listed in the top panel. The future participants are listed in the top panel. The future participants are listed in the top panel. The future participants are listed in the top panel.

SOLA-06

2012

CEDAR

2013



June 22 - June 28

Millenium Hotel - Boulder, Colorado





2013



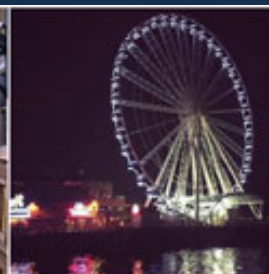
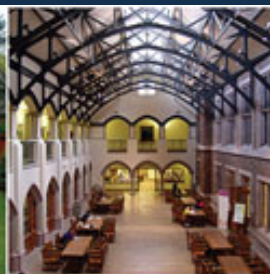
Barbara Emery
NCAR / 1000

H-K
BANKERS BOX

2013



2013

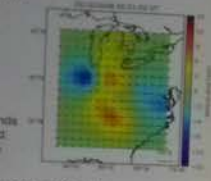


June 22 - June 26, Seattle
University of Washington



2014





DATA-01

A Data Assimilative Comparison of Solar Cycle 24 Magnetic Storms
G.S. Bust, JHUAPL and K.H.E. Slaathaug, La Conner, WA

DATA-01



Introduction

- DAAD is used compare and contrast six different storms from the most recent solar cycle.
- Global storm properties are characterized by hemispheric power and Dist.
- The response of each storm is compared to the global storm characteristics and to each other.
- Of particular interest are unusual or interesting ionospheric structures and their correlation to the global storm properties.

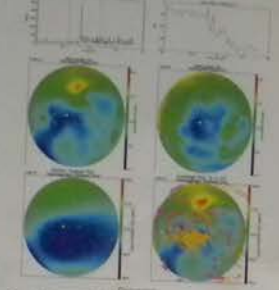
Overall Objectives

- We will compare the storms to each other to improve our understanding of storm-time variability.
- We will contrast the ionosphere pre-storm coast to the ionospheric response after storm onset, and we will study the variability of this response between storms.

Approach

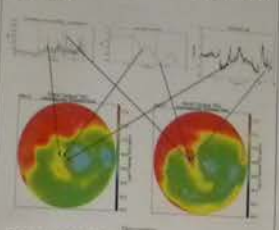
To estimate the global 3D time-evolving ionosphere for each storm, TEC plots, and electron density profiles were made at various altitudes. The plots were taken from the IRI model and/or unusual spatial structures were compared with other storms and with Dist and hemispheric power.

2010095: 9-11 UT: Enhancement in Southern hemisphere



- The enhancement in TEC occurs in the southern polar region of 70-80 UT -100 magnetic latitude and near MLT noon.
- It appears to be associated with the large hemispheric power input at 78 UT.
- It does not appear in the northern hemisphere. Why?
- Is due to IRI model not due to lack of data.
- Localized power input - specific latitude / time?

2011069: Relation between hemispheric power input, changes in Dist and polar plasma structuring



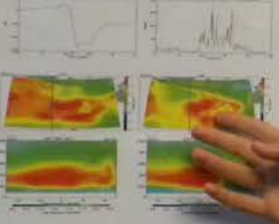
- Polar plots at 9:40 UT (Dist) is associated with lower power increase in hemispheric power and positive decrease in Dist.
- Later at 11:40 a second polar lobe of ionospheric power and Dist is associated with structuring extends over entire polar cap to night side sector. After associated with increase in hemispheric power and decrease in Dist.
- The Dist enhancement is due to a rise when it is just coming toward the south after being south for several hours.
- The second enhancement storm after a 10 hour time continued turning and then it turns south again.

2011217: High altitude plasma transported across pole



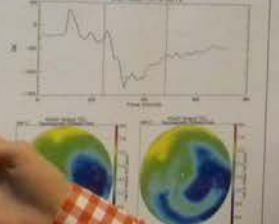
- Upper left plot is 100 km electron density.
- Lower left plot is 100 km electron density.
- Right plot is 100 km electron density.
- High altitude plasma transport across pole.
- Electron density profiles.

2012069: Extension of polar plasma over USA



- There is a pre-storm enhancement in the southern USA region? At 0:00.
- At 3:30 UT (shown top right) it is represented as a narrow channel of the plasma from the southern USA (Florida effect) extending as far west as Washington.
- At 4:00 UT (shown bottom right) it is represented as a narrow channel of the plasma from the southern USA (Florida effect) extending as far west as Washington.
- The lower left and right plots show altitude versus latitude of electron density. The right hand plot shows the primary region extending to higher altitudes.

2013275: Enhanced E-region



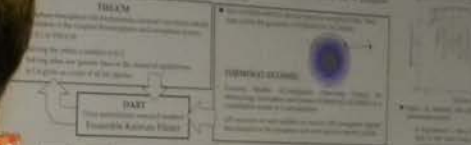
- There is a pre-storm enhancement in the southern USA region? At 0:00.
- At 3:30 UT (shown top right) it is represented as a narrow channel of the plasma from the southern USA (Florida effect) extending as far west as Washington.
- At 4:00 UT (shown bottom right) it is represented as a narrow channel of the plasma from the southern USA (Florida effect) extending as far west as Washington.
- The lower left and right plots show altitude versus latitude of electron density. The right hand plot shows the primary region extending to higher altitudes.

DATA-03

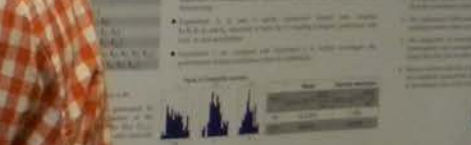
Effects of inferring unobserved Thermospheric and Ionospheric parameters using an Ensemble Kalman Filter on global Ionospheric Specific

Abstract | We have assessed the impact of inferring unobserved thermospheric and ionospheric parameters using an ensemble Kalman filter (EnKF) on global ionospheric specific parameters...

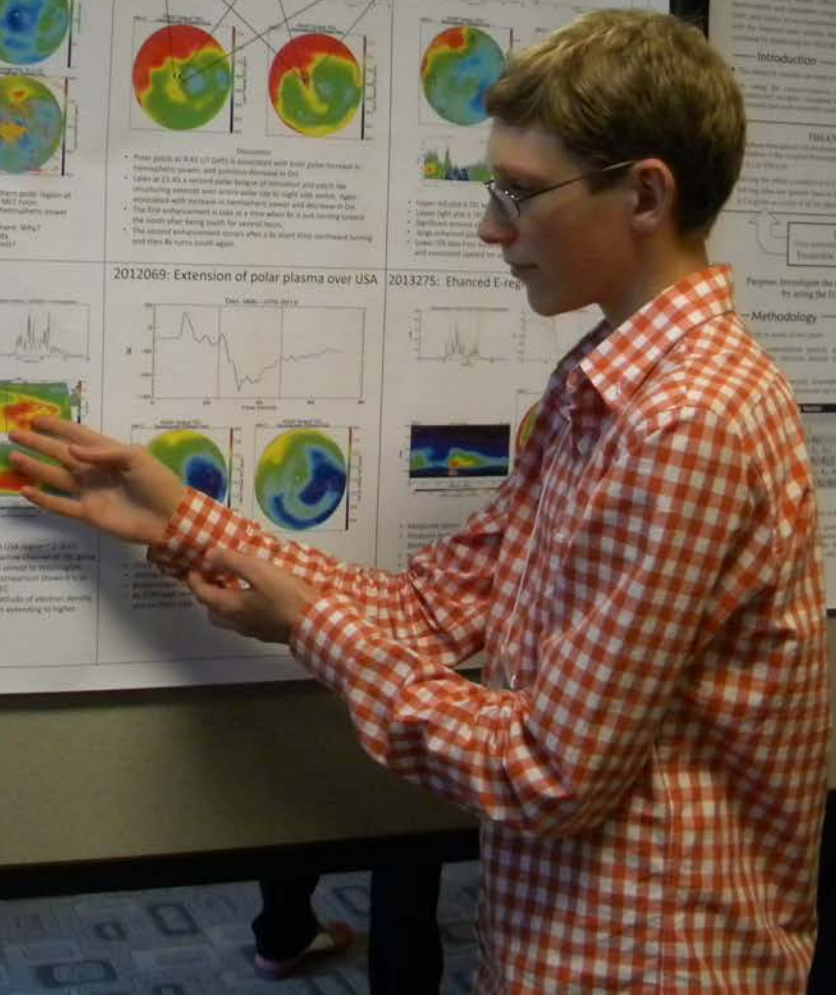
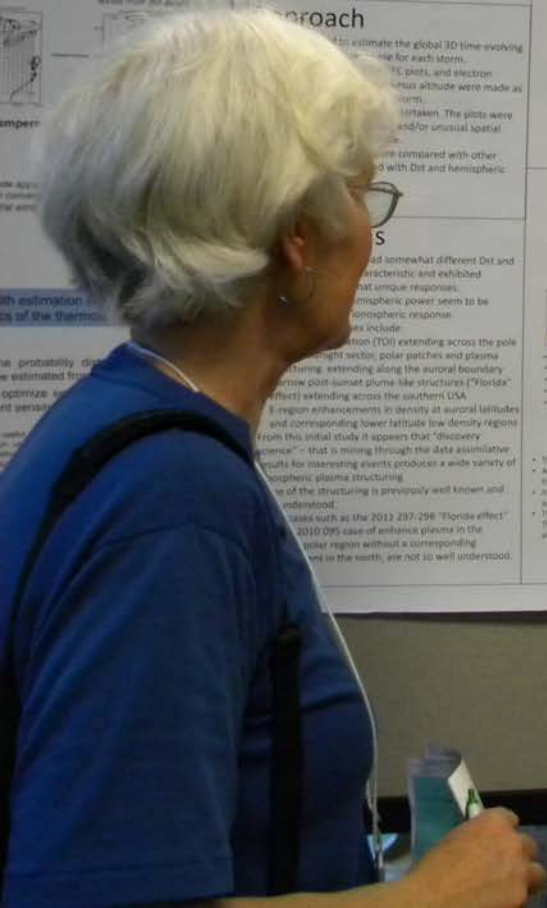
Introduction | The EnKF is a data assimilation technique that allows for the simultaneous estimation of model parameters and states...



Methodology | We used the EnKF to estimate the global ionospheric specific parameters from a set of observations...



Conclusions | The EnKF provides a robust and accurate method for inferring unobserved thermospheric and ionospheric parameters...



CEDAR 2015



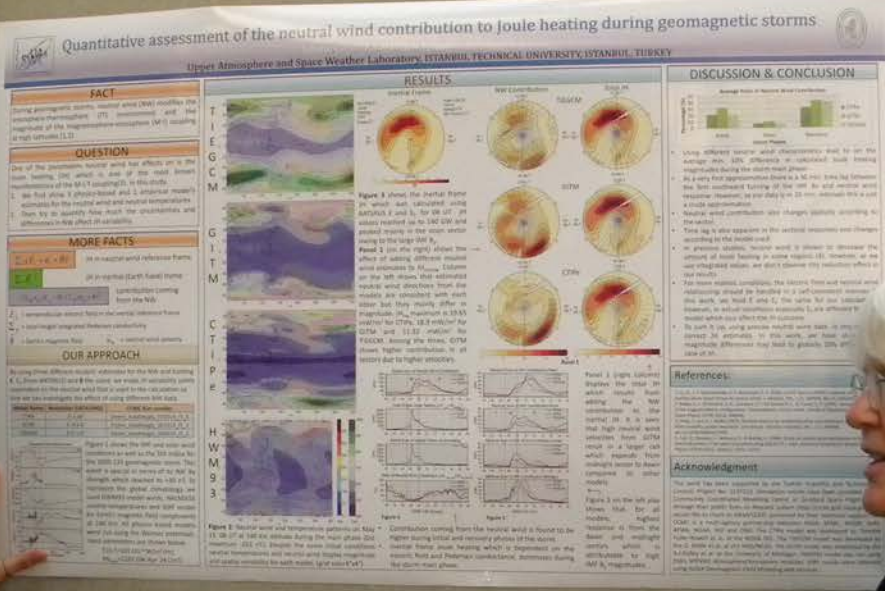
June 21 - June 25, Seattle
University of Washington





2015

SOLA-08



SOLA-07

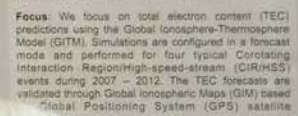
Towards Forecasting

Xing Meng, A
Jet Pro

INTRODUCTION

Motivation: Conditions in the ionosphere have become increasingly important to forecast, since more and more spaceborne and ground-based technological systems rely on the ionosphere. The current generation of physics-based global ionospheric models is adequately advanced to permit an analysis of forecasting.

Focus: We focus on total electron content (TEC) predictions using the Global Ionosphere-Thermosphere Model (GITM). Simulations are configured in a forecast mode and performed for four typical Corotating Interaction Region/High-speed-stream (CIR/HSS) events during 2007 – 2012. The TEC forecasts are validated through Global Ionospheric Maps (GIM) based on Global Positioning System (GPS) satellite



aim to understand the model behavior long-term ionospheric forecasts.



- Forecast performance**
- The forecast is generally good.
 - The forecast is generally good.
 - The forecast is generally good.
 - The forecast is generally good.

2015



Richard Behrke

C
E
D
A
R

CEDAR
1999
Fourth Summer Workshop

2015



2015



2015



CEDAR-GEM JOINT WORKSHOP



19 - 24 JUNE 2016 ~ SANTA FE, NEW MEXICO

UNIVERSITY OF LOUISVILLE

Long-lasting Mesospheric Inversion Layers in eCMAM30

Christian A. Tate and Jian Du (cdtate01@louisville.edu)
Department of Physics and Astronomy, University of Louisville, Kentucky

Abstract

Mesospheric inversion layers (MILs) are widely studied phenomena that reverse the usual temperature-altitude gradient due in part to planetary wave breaking and/or tides. This investigation uses the extended Canadian Middle Atmosphere Model (eCMAM30) for years 1997-2009 of dynamic and chemical data to explore the temperature and altitude distributions of long-lasting (>3 days) MILs. The temporal and spatial trends of MIL events are synoptically examined. Being the first time eCMAM30 is used to study the distributions of MILs events, this analysis presents an timely opportunity to compare results with other general circulation models. In agreement with WACCM (Fritzsche et al. 2015) and lidar observations (Gao et al. 2012, Mervinther and Gerrard 2004), the eCMAM30 data-set shows similar trends in low and middle latitudes with the seasonal variability most dominant in the tropics during the equinoxes. The distribution of temperature, thickness, duration and scale are also examined. The results show that breaking to elucidate the mechanisms of long-lasting MILs as they occur.

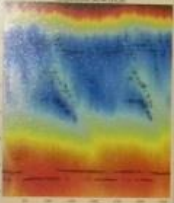
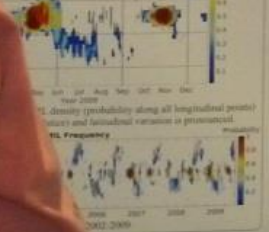


Figure 2. Altitude-time heat-step of temperature, with tropopause (dotted) and MIL top/bottom (crosses).

Data and Methods of MILs

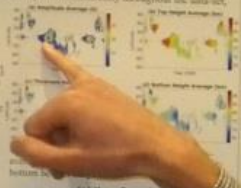
In order to elucidate the statistical trends of long-lasting MIL events in the extended Canadian Middle Atmosphere Model, a MIL event is a temperature inversion layer that satisfies the condition: $\Delta T > 10$ K and $\Delta z > 4$ km. The altitude must be below the mesopause and above the tropopause as shown in Figure 2. MILs must have a temperature-increasing lapse rate. The amplitude (temperature inversion) must be greater than 10 K and the altitude scale of the temperature inversion greater than 4 km. See crosses in Figure 2 and blue dots in Figure 3.

MILs persist over at least three of averaged temperature data.



Time and Latitudinal Dependence

When MIL events are longitudinally averaged (Figures 3, 4 and 5), their distributions show strong seasonal and latitudinal dependences. In Figure 3 the tropical equinoxes (March/September) gradually increase and decrease in MIL density, peaking at 100% for the entire equatorial zone. At a given longitude MIL events can last up to 30 days. The solstices (June/December) show "wings" extending from the tropics into the middle latitudes of the winter hemisphere. Figure 4 shows this pattern consistently throughout the data-set, except when the spring equinox events are diminished every other year—most likely due to the quasi biennial oscillation (Garcia, 1997) (Figure 5a) and (c) follow similar trends as the MIL density as Figure 3. Figure 5(b), 5(d) and 2 show the downward evolution of MIL events.



(a) Year-Round

(b) Equinoxes

(c) Solstices

The Time averaged MIL densities for years 1978-2009 as Figure 6 show strong longitudinal and latitudinal trends. Long-lasting MIL events occur most frequently during the equinox seasons in the tropics, meaning that they are most likely tidally driven. The solstice events, however, primarily occur in the middle latitudes as shown in Figures 3, 4 and 6(c). Note the non-migrating tides in the tropics and middle latitudes. Also note that there are much fewer MIL in the Antarctic, even though the two hemispheres has an equal number of MIL events in total. Figure 10 shows that Arctic MIL events have greater amplitudes and thicknesses—a sign of planetary wave phenomena.

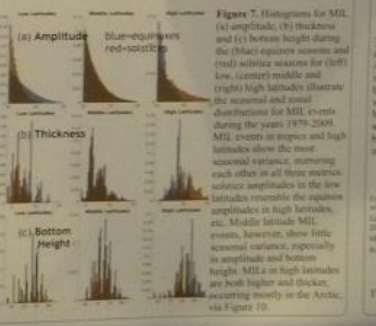


Figure 6. Latitude-longitude map of MIL density (row arranged) for 1997-2009 (a) year-round, (b) equinox and (c) solstice seasons.

Figure 7. Histograms for MIL (a) amplitude, (b) thickness and (c) bottom height during the (left) equinox seasons and (right) solstice seasons for (left) low, (center) middle and (right) high latitudes illustrate the seasonal and spatial distributions for MIL events during the years 1978-2009. MIL events in tropics and high latitudes show the most seasonal variance, occurring each other as all three metrics solstice amplitudes in the low latitudes resembles the equinox amplitudes in high latitudes, etc. Middle latitude MIL events, however, show little seasonal variance, especially in amplitude and bottom height. MILs in high latitudes are both higher and thicker, occurring mostly in the Arctic, via Figure 10.

A comparison of statistical characteristics of the diurnal tide and illustrate how these characteristics change with season, latitude and altitude from the troposphere to the thermosphere/mesosphere using data from the extended Canadian Middle Atmosphere Model (eCMAM30) for 1978-2010 and the Sounding of the Atmosphere using Broadband Emission Radiometry (SABER) instrument on NASA's TIMED (Thermosphere Ionosphere Mesosphere Energetics Dynamics) satellite.

The poster show the comparison of statistical properties (correlations and probability density functions) of short-term and long-term tidal variability of migrating tide (DW1) as a function of time, height, altitude, and latitude between eCMAM30 and SABER. Wavelet analysis is used to examine the underlying statistics governing the short-term tidal variability and to what extent these PSDs changes temporally and spatially and apply to the thermospheric situation to study physical mechanism.



Figure 1. Day-to-day variation of DW1 T amplitude at the equator in year 2007 for eCMAM30 (left) and SABER (right).

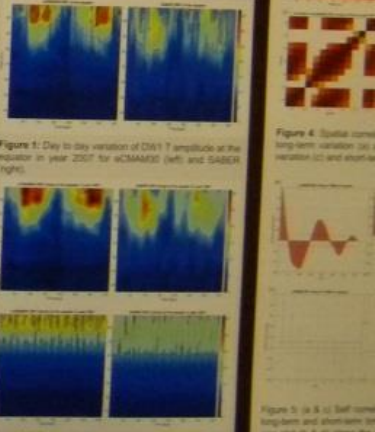


Figure 2. Top: Long-term variation (30 days) and (Bottom) short-term variation (3-5 days) of DW1 T amplitude at the equator in year 2007 for eCMAM30 (left) and SABER (right).

argest buoyantly driven convective mode
Cosslette¹, Mark Rast²
Space Physics, University of Colorado, Boulder
Sciences, Laboratory for Atmospheric and Space Physics,
of Colorado, Boulder



Preserving a Unique Archive for Long-Term Solar Variability Studies
Newitts, L¹, R. McAdoo¹, B. L. ...
¹SP, Boulder College, Chestnut Hill, MA; ²ADACAR, Boulder, CO; ³Atmospheric and Environmental Sciences, University of Colorado, Boulder

BACKGROUND AND MOTIVATION

ORBITING AND

PUBLICITY

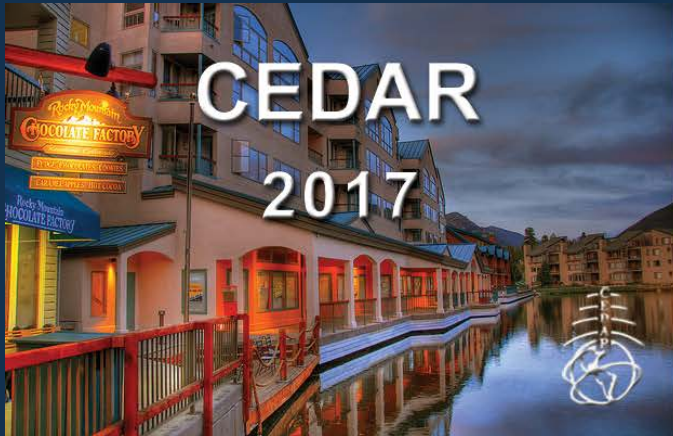


2016



2016

CEDAR 2017



18 - 23 June
Keystone Resort, Colorado